MBNA Publishing House Constanta 2021

Proceedings of the International Scientific Conference SEA-CONF

SEA-CONF PAPER • OPEN ACCESS

Algorithm-based methods as information source for plasma – material interaction studies- an overview

To cite this article: Valentina MARASCU and Anca BONCIU, Proceedings of the International Scientific Conference SEA-CONF 2021, pg.252-259.

Available online at www.anmb.ro

Algorithm-based methods as information source for plasma – material interaction studies- an overview.

Valentina Marascu [1, 2, *] **and Anca Bonciu** [1, 3]

[1] National Institute for Laser, Plasma and Radiation Physics, RO-077125 Magurele, Romania.
[2] Université Paris-Saclay, CEA, INRAE, DMTS, SCBM, F-91191 Gif-sur-Yvette, France.
[3] Faculty of Physics, University of Bucharest, RO-077125 Magurele, Romania.
*Corresponding author: valentina.marascu@gmail.com

Abstract. Algorithm-based methods represent a useful tool, for information extraction, offering in the same time a new perspective of the obtained results. In our paper, we exposed an overview of the applied, manual and automatic, algorithm-based methods, in order to investigate the outcome of plasma-material interactions. Briefly, Hough Transform, Canny edge detection, and circularity analyses were applied on images. In this line, the information was extracted from Scanning Electron Microscopy (SEM) images. Hereon, statistical analyses were performed for various experimental parameters in order to formulate valuable conclusions.

1. Introduction

Information occurs in every domain, being in the same time a priceless instrument for our daily existence. Hereinafter, computer science approaches play an important role for its encoding or decoding approaches [ref.1; ref.2; ref.3]. Briefly, we are surrounded by information, from symbols, up to physical phenomena, and the list does not stop here. In order to be completely understood, the encoded information must be further processed. The diversity and complexity of decoding methods exceed the expectations each time; methods that are expressed via various and novel algorithms.

In plasma physics domain, the needs of algorithms, for information extraction, increase each day. One can highlight the use of plasma in various domains, e.g., plasma-based engines for space propulsions [ref.4], anticorrosive coatings for in naval diesel engines, obtained via plasma methods [ref.5], etc. In this line, plasma – material interaction, represents a particular field. Though, the need of accurate results is related due to the progress of fusion facilities, like ITER, SPARC, DEMO, and so on. These facilities are/ will be operationally in the nearest future, having the main scope to produce clean energy, by using a thermonuclear plasma [ref.6; ref.7; ref.8]. One of the many concerns about plasma operation, is related with its interaction with the inside vessel walls. Simulation had shown various phenomena, which will conduct to melting and new-material formation, contaminating in the same time the plasma discharge.

Our experimental approach in this paper, includes lab-scale plasma-material interaction. Hereon, the used material was Tungsten, which is well known for its important properties, like high melting point (~3400º C), low sputtering rates, electrochemical properties, and having multiple applications, from fusion domain (e.g., divertor region in ITER) [ref.9], up to defense (e.g., high kinetic energy penetrator, small caliber ammunition) [ref.10; ref.11]. Further, an atmospheric pressure plasma jet (Microjet discharge) interacted with Tungsten material, leading to particles formation [ref.12; ref.13].

The resulted particles were investigated via Scanning Electron Microscope (SEM), in order to obtain grey scale images.

In our previous papers [ref.12; ref.13], one has shown a statistical description of tungsten particles, by analyzing SEM images via ImageJ software, in manual mode. The resulted size distributions showed a correlation between the plasma input power and the particles size, meaning that for higher power we obtained bigger particles.

In this line, our current paper emphasis an overview of our previous results, between manual mode detection [ref.12; ref.13], and automatic image detection [ref.14], for particles characterization obtained after plasma treatment. Following this method, one can extract the needed information related to particles characterization.

2. Results and discussions

Particle's detection process implies two parts: in the first part, tungsten particles obtained in plasma are measured in SEM instrument, obtaining SEM images. In the second part, SEM images are processed in order to detect particle's size, due to algorithm-based methods, which are described further on. Briefly, tungsten particles detection implies the manipulation of SEM images. Nevertheless, additional processing is needed, e.g., to remove the unwanted pixels, to adjust the illumination, depending exclusively on the measured material (in our case, tungsten particles).

One can observe that the number of pre-processing methods of the desired images, is strongly related with the unusual phenomena that can occur during material analyses inside the microscope.

Particularly, automatic particles detection was used for analyze the initial and plasma treated polystyrene sphere experiments [ref.14]. This it's an example of detecting particles arranged in 1-level on the substrate surface. Briefly, SEM images of the initial and plasma treated polystyrene spheres, were filtered in order to reduce the unwanted pixels, followed by threshold conversion of the images. Further, circular Hough transform was applied. Because polystyrene spherical-like particles were arranged in 1-level on the substrate, it was possible to apply the squared modulus of the 2D-FFT, in order to establish the uniform/ non-uniform distribution of the polystyrene spheres on the substrate [ref.14]. In Figure 1 is presented a schematical view of the automatic SEM image processing of the initial and plasma treated polystyrene spheres.
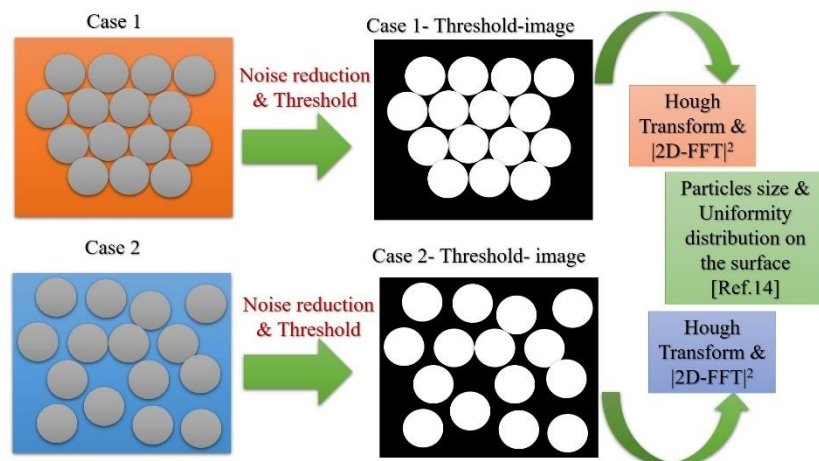
Figure 1: Steps for automatic particles detection via Hough transform & uniformity studies via squared modulus of 2D-FFT.

2.1. Tungsten particles detection via manual image processing method

In our previous papers [ref.12; ref.13], tungsten particles detection was made via manual mode, by using ImageJ. Herein, SEM images were analyzed one by one, being rescaled in microns scale. This step is possible by using the scale provided by the SEM microscope internal parameters. Further, each eye-detectable particle was measured (diameter measurement), manually, as it can be observed bellow (Figure 2). The obtained diameters were exported in ASCII files, and imported in OriginLab Software for statistical descriptions.
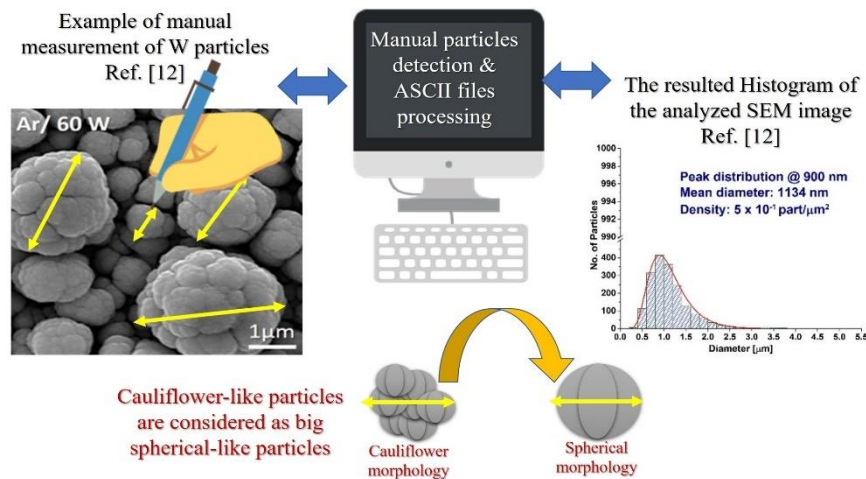
Figure 2: Schematical view of the manual particle's detection.

Thus, a global restriction was used in this approach: cauliflower-like morphology was considered as a spherical-like morphology. Meaning, one has neglected the existence of the smaller particle's morphologies. Cauliflower-like morphology is made by smaller individual particles, which are attached together to form one big particle, in the coldest region of the plasma.

It's not the recommended approach at all, for a higher amount of particles detection, due to time consuming. One can chose the manual method in case of multi-level particles arrangement, with particles having close pixels values. As a result, the particles were detected and size distributions were performed, by using a measurement surfaces of 3520 μm^2 [ref.12] and 35.52 μm^2 [ref.13].

One can observe an increase of the particles size in relation with the input power, for higher surface detection (3520 μm^2 [ref.12]). Further on, measuring the particles, made via Microjet discharge, in Argon atmosphere, by applying an input power between 20W-100W [ref.12], the mean particles diameter starts from 462 nm [ref.12] up to 4365 nm [ref.12]. One can conclude the influence of the input power regarding tungsten particles synthesis: increasing the input power, the plasma interacts strongly with tungsten material, producing a higher amount of tungsten metallic vapors.

Having in mind the obtained cauliflower like morphologies, it can be suggested that the metallic vapors are suspended in the plasma jet for a longer time, interacting with further condensed particles, forming bigger cauliflower like morphologies. In the second approach, by investigating a smaller surface area (35.52 μm^2 [ref.13]) one can observe a correlation between the distance of the plasma source and the substrate. In this approach one can conclude that by using a distance of 6mm (between substrate and plasma source), one can obtain particles with a mean diameter between 157 nm -176 nm, depending of the used plasma source geometry [ref.13]. More experimental details and discussions can be consulted in ref.12 and ref.13.

2.2. Tungsten particles detection via automatic image processing method

In the following approach, were selected SEM images of tungsten particles obtained via microjet, in argon atmosphere (1 atm), for the following input powers: 20W; 40W; 60W; 80W; 100W [ref. 12]. The method implies image processing in 5 steps. An important aspect is to obtain a uniform illumination of the image. This unusual phenomenon is related to SEM instrument limitations.

SEM image processing method involves several steps: first, initial image is opened. Step 1- Step 3 starts by applying a correction of the luminosity (via *imadjust* function [ref.15]), and extracting the background from the initial SEM image. Step 4 continue the processing, by applying an adaptive threshold (via *adaptthresh* function [ref.16]). Further on, in Step 5 one fill (via *imfill* function [ref.17]) the thresholded image, in order to obtain a complete geometry of the particles. Thus, this approach is time consuming, but do not imply high computational resources, and can be adjust very easily to a high variety of SEM images. The code description of the first 5 Steps is shown below (the case of SEM images for particles obtained at 60W).

-- *code description for SEM image loading & processing:*

```matlab
clear all;
clear clc;
clc;
% image loading
SEM = imread (uigetfile('*.*'));
SEM_gray = rgb2gray(SEM);
figure (1)
imshow (SEM_gray)
title('Initial SEM image')
    % non-uniform ilumination correction
    SEM_gray_2 = strel('disk',20);
    background = imopen(SEM_gray,SEM_gray_2);
    figure (2)
    imshow(background)
    title('Background of the initial SEM image')
        %imwrite(background,'Background of the initial SEM image @ 20W_STEP 2.jpg');
        %imwrite(background,'Background of the initial SEM image @ 40W_STEP 2.jpg');
    imwrite(background,'Background of the initial SEM image @ 60W_STEP 2.jpg');
        %imwrite(background,'Background of the initial SEM image @ 80W_STEP 2.jpg');
        %imwrite(background,'Background of the initial SEM image @ 100W_STEP 2.jpg');
C = SEM_gray - background;
figure (3)
imshow(C)
title('Resulted SEM image')
        %imwrite(C,'Resulted SEM image @ 20W_STEP 3.jpg');
        %imwrite(C,'Resulted SEM image @ 40W_STEP 3.jpg');
    imwrite(C,'Resulted SEM image @ 60W_STEP 3.jpg');
        %imwrite(C,'Resulted SEM image @ 80W_STEP 3.jpg');
        %imwrite(C,'Resulted SEM image @ 100W_STEP 3.jpg');
    C_1= imadjust(C);
    figure (4)
    imshow(C_1)
    title('Uniform-Luminosity SEM image')
        %imwrite(C_1,'Uniform-Luminosity SEM image @ 20W_STEP 4.jpg');
        %imwrite(C_1,'Uniform-Luminosity SEM image @ 40W_STEP 4.jpg');
```

```
                    imwrite(C_1,'Uniform-Luminosity SEM image @ 60W_STEP 4.jpg');
                       %imwrite(C_1,'Uniform-Luminosity SEM image @ 80W_STEP 4.jpg');
                       %imwrite(C_1,'Uniform-Luminosity SEM image @ 100W_STEP 4.jpg');
% SEM treshold
D = adaptthresh(C_1, 0.6);
E = imbinarize(C_1,D);
figure (5)
imshow (E)
title('Tresholded SEM image')
                       %imwrite(E,'Tresholded SEM image @ 20W_STEP 5.jpg');
                       %imwrite(E,'Tresholded SEM image @ 40W_STEP 5.jpg');
                    imwrite(E,'Tresholded SEM image @ 60W_STEP 5.jpg');
                       %imwrite(E,'Tresholded SEM image @ 80W_STEP 5.jpg');
                       %imwrite(E,'Tresholded SEM image @ 100W_STEP 5.jpg');
% Fill particles
    F = imfill(E, 'holes');
    figure (6)
    imshow (F)
    title('Fill holes from Tresholded SEM image')
                       %imwrite(F,'Fill holes from Tresholded SEM image @ 20W_STEP 6.jpg');
                       %imwrite(F,'Fill holes from Tresholded SEM image @ 40W_STEP 6.jpg');
                    imwrite(F,'Fill holes from Tresholded SEM image @ 60W_STEP 6.jpg');
                       %imwrite(F,'Fill holes from Tresholded SEM image @ 80W_STEP 6.jpg');
                       %imwrite(F,'Fill holes from Tresholded SEM image @ 100W_STEP 6.jpg');
```

-- end of first selected section [ref.15], [ref.16], [ref.17].

After SEM image processing, circular Hough transform was applied via *imfindcircles* function [ref.18]. By inserting a minimum radius (10 pixels in our example), and a maximum radius (14 pixels), one can detect all circles in this range. For higher radii detection, one can simply complete with further minimum and maximum radii intervals. The following attributes *'ObjectPolarity', 'bright', 'sensitivity',* and *'edge threshold'* defines the fact that circular Hough transform is applied on bright objects (in our case, white particles geometries), with a higher accuracy (expressed by the value added to *sensitivity* attribute), and a strong boundary (0.4 value for edge threshold attribute).

-- Particles detection via circular Hough Transform- selected section from the program:

```
% particles detection in the adjusted image for 60W
    [centersBright,radiiBright]=imfindcircles(F,[10
14],'ObjectPolarity','bright','Sensitivity',0.94,'EdgeThreshold',0.4);
        viscircles(centersBright, radiiBright,'Color','b'); % small particles
```

-- end of the second selected section [ref.18], [ref.19] and [ref.20].

Figure 3 highlights an example of SEM image processing, and particles detection. In Figure 4, one can observe the obtained statistical description for all automatic particle detection in SEM images, obtained at input powers between: 20W – 100W.
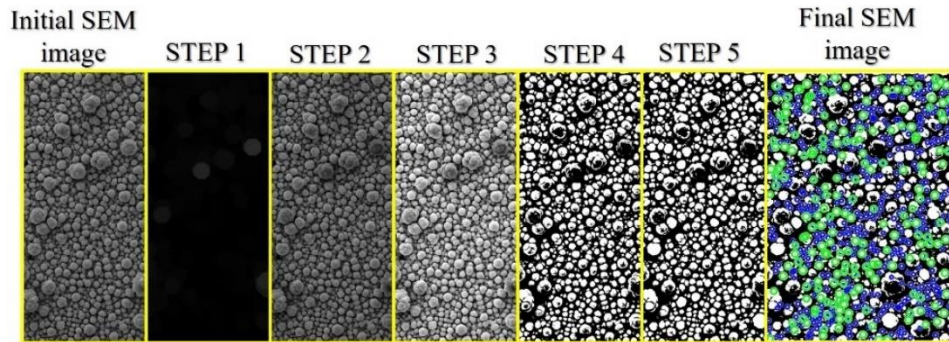
Figure 3: Example of SEM image processing and particles detection for W particles obtained at 60W.

Comparing with the results from our previous paper [ref.12], one can highlight two general statements: first, in both cases (in current paper and in ref.12) we have used an area of 3520 μm^2. Second, while in ref.12 we had considered the cauliflower-like morphology as being spherical-like morphology (explained in *section 2.1*), in the current paper one had considered the cauliflower morphology as being formed from smaller spherical-like morphologies. As consequence, one resulted double histogram, in the case of analyzing SEM images corresponding to W particles obtained at 40W, 60W and 100W. That suggest the existence of two categories of particles: smaller and medium particles. Herein, one can consider a big particle is formed from small and medium particles.

Due to initial particles geometry considerations, canny edge detection will conduct to various lines of the cauliflower morphology, resulting a curves map only for one big particle. In addition, canny approach cannot be implemented for our material. Further on, circularity calculation (e.g., a circular object has a value equal to 1) cannot be considered, due to same cauliflower-like morphologies issue.
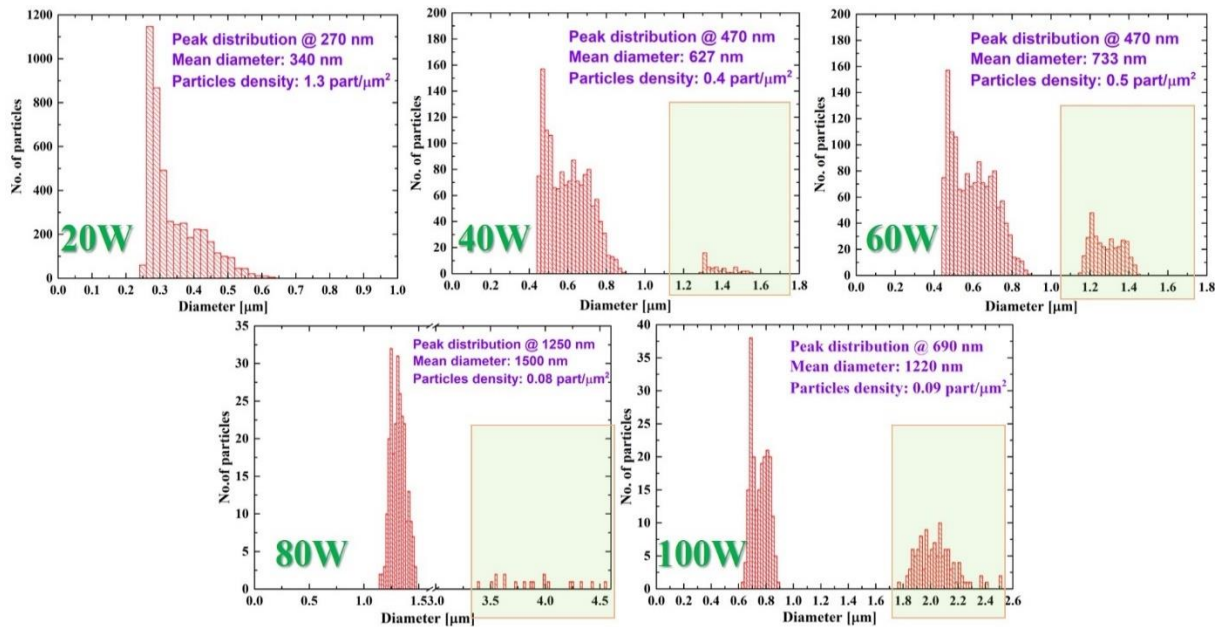
Figure 4: Statistical description of the processed SEM images.

3. Conclusions

Particles were automatically detected via image processing methods. The studied material were tungsten particles, obtained by a microjet plasma, in argon discharge, by applying different input powers (20W – 100W) [ref.12]. One has considered the cauliflower-like morphology, as being formed from little spherical-like morphologies coupled together. In this line, one can described the componence of the bigger particles. This approach it can be seen as complementary to that described in ref.12, and also, which was explained in the current paper.

One described a method of analyzing particles from SEM images, in 5 steps. On the final SEM image processing step, circular Hough transform was applied in order to detected the radii of its. Thus, due to morphological constraints of the analyzed particles, canny method and circularity characterization were not possible to be used.

The obtained size distributions (e.g., histogram, in figure 4), showed an interesting density of the measured particles: at a low input power (20W) tungsten particle are numerous and with small sizes, while for high input power (100W), one can observe a double histogram with a low particle's density. Suggesting that during particles formation in plasma, a higher input power leads to a higher melting of the exposed material, obtaining big particles formed from smaller particles.

Further investigations will concern the formation of particles inside the plasma discharge.

References
[1] Nita, S.L.; Mihailescu, M.I.; Pau, V. C. *Security and cryptographic challenges for authentication based on biometrics data*, MDPI Cryptography 2018 2(4): 39. https://doi.org/10.3390/cryptography2040039 .

[2] Nita, S. L.; Mihailescu, M.I. *On Artificial Neural Network used in Cloud Computing Security - A Survey*, 10th International Conference on Electronics, Computers and Artificial Intelligence (ECAI), Iasi, Romania, 2018, pp. 1-6. DOI: 10.1109/ECAI.2018.8679086.

[3] Nita, S.L.; Mihailescu, M.I. *A hybrid searchable encryption scheme for cloud computing* (2019) In: Lanet JL., Toma C. (eds) Innovative Security Solutions for Information Technology and Communications. SECITC 2018. Lecture Notes in Computer Science, vol. 11359, Springer, Cham. https://doi.org/10.1007/978-3-030-12942-2_8 .

[4] Franklin R. Chang-Diaz, *Plasma propulsion for interplanetary flight*, Thin Solid Films 506– 507 (2006) 449 – 453. doi:10.1016/j.tsf.2005.08.324 .

[5] Baiamonte, L.; Marra, F.; Gazzola, S.; Giovanetto, P.; Bartuli, C.; Valente, T.; Pulci, G. *Thermal sprayed coatings for hot corrosion protection of exhaust valves in naval diesel engines*, Surface & Coatings Technology 295 (2016) 78–87. http://dx.doi.org/10.1016/j.surfcoat.2015.10.072

[6] Bigot, B ., *ITER assembly phase: Progress toward first plasma*, Fusion Engineering and Design 164 (2021) 112207. https://doi.org/10.1016/j.fusengdes.2020.112207

[7] Creely, A. J.; et al., *Overview of the SPARC tokamak*, J. Plasma Phys. (2020), vol. 86, 865860502. doi:10.1017/S0022377820001257.

[8] Bachmann, C.; et al., *Initial DEMO tokamak design configuration studies*, Fusion Engineering and Design 98–99 (2015) 1423–1426. http://dx.doi.org/10.1016/j.fusengdes.2015.05.027

[9] Pitts, R.A., et al, *A full tungsten divertor for ITER: Physics issues and design status*, Journal of Nuclear Materials, Volume 438, Supplement, July 2013, Pages S48-S56. https://doi.org/10.1016/j.jnucmat.2013.01.008.

[10] Koutsospyros, A.; Braida, W.; Christodoulatos, C.; Dermatas, D.; Strigul, N. *A review of tungsten: From environmental obscurity to scrutiny*, Journal of Hazardous Materials, Volume 136, Issue 1, 10 August 2006, Pages 1-19. https://doi.org/10.1016/j.jhazmat.2005.11.007

[11] Ji-cheng Li; Xiao-wei Chen; Feng-lei Huang, *Ballistic performance of tungsten particle / metallic glass matrix composite long rod*, Defence Technology, Volume 15, Issue 2, April 2019, Pages 132-145. https://doi.org/10.1016/j.dt.2018.06.009.

[12] Marascu, V.; Stancu, C.; Satulu, V.; Bonciu, A.; Grisolia, C.; Dinescu, G. *Material erosion and*

dust formation during tungsten exposure to Hollow-Cathode and Microjet Discharges, Applied Sciences-Basel, Volume: 10, Issue: 19, Article Number: 6870, Published: OCT 2020. https://doi.org/10.3390/app10196870.

[13] Marascu, V.; Lazea-Stoyanova, A.; Bonciu, A.; Satulu, V.; Dinescu, G. *Tungsten particles fabrication by a microjet discharge*, Materials Research Express, Volume: 7, Issue: 6, Article Number: 066509, Published: JUN 2020. https://doi.org/10.1088/2053-1591/AB955D.

[14] Marascu, V.; Chitescu, I.; Barna, V.; Ionita, M. D.; Lazea-Stoyanova, A.; Mitu, B.; Dinescu, G. *Application of image recognition algorithms for statistical description of nano- and microstructured surfaces*, 9th International Physics Conference Of The Balkan Physical Union (BPU-9), Book Series: AIP Conference Proceedings, Volume: 1722, Article Number: 290006, Published: 2016. https://doi.org/10.1063/1.4944292

[15] https://se.mathworks.com/help/images/ref/imadjust.html?searchHighlight=imadjust%20&s_tid=srchtitle

[16] https://se.mathworks.com/help/images/ref/adaptthresh.html?searchHighlight=adaptthresh&s_tid=srchtitle

[17] https://se.mathworks.com/help/images/ref/imfill.html?searchHighlight=imfill&s_tid=srchtitle

[18] https://se.mathworks.com/help/images/ref/imfindcircles.html

[19] https://se.mathworks.com/help/images/ref/viscircles.html

[20] https://fr.mathworks.com/help/images/detect-and-measure-circular-objects-in-an-image.html